

# Human labeling errors and their impact on ConvNets for satellite image scene classification

Longkang Peng<sup>a,b</sup>, Tao Wei<sup>a,\*</sup>, Xuehong Chen<sup>c</sup>, Xiaobei Chen<sup>a,b</sup>, Rui Sun<sup>a</sup>, Luoma Wan<sup>b</sup>, Xiaolin Zhu<sup>b</sup>

<sup>a</sup> School of Psychology, Shenzhen University, Shenzhen 518060, China

<sup>b</sup> Department of Land Surveying and Geo-Informatics, The Hong Kong Polytechnic University, Hong Kong, China

<sup>c</sup> State Key Laboratory of Remote Sensing Science, Faculty of Geographical Science, Beijing Normal University, Beijing 100875, China

\*Corresponding author:

Tao Wei

Email: tao.wei@szu.edu.cn

## Abstract

Convolutional neural networks (ConvNets) have been successfully applied to satellite image scene classification. Human-labeled training datasets are essential for ConvNets to perform accurate classification. Errors in human-labeled training datasets are unavoidable due to the complexity of satellite images. However, the distribution of human labeling errors on satellite images and their impact on ConvNets have not been investigated. To fill this research gap, this study, for the first time, collected real-world labels from 32 participants and explored how their errors affect three ConvNets (VGG16, GoogleNet and ResNet-50) for high-resolution satellite image scene classification. We found that: (1) human labeling errors have significant class and instance dependence, which is fundamentally different from the simulation noise in previous studies; (2) regarding the overall accuracy of all classes, when human labeling errors in training data increase by one unit, the overall accuracy of ConvNets classification decreases by approximately half a unit; (3) regarding the accuracy of each class, the impact of human labeling errors on ConvNets shows large heterogeneity across classes. To uncover the mechanism underlying the impact of human labeling errors on ConvNets, we further compared it with two types of simulated labeling noise: uniform noise (errors independent of both classes and instances) and class-dependent noise (errors independent of instances but not classes). Our results show that the impact of human labeling errors on ConvNets is similar to that of the simulated class-dependent noise but not to that of the simulated uniform noise, suggesting that the impact of human labeling errors on ConvNets is mainly due to class-dependent errors rather than instance-dependent errors.

**Keywords:** label noise, human labeling error, convolutional neural network, satellite image scene classification

## 1. Introduction

Convolutional neural networks (ConvNets) based on supervised learning paradigm have repeatedly achieved great performance across a variety of computer-vision tasks in different domains (Khan et al., 2020, 2022), including in the remote sensing domain (Ball et al., 2017). Based on the supervised learning paradigm, ConvNets learn from labeled training data to perform well in real-world tasks (Liu, 2011). In this context, the quality of the training data is essential for the performance of ConvNets (Zhu and Wu, 2004). Nevertheless, the training data collected for real-world tasks frequently contains errors in their labels (Nettleton et al., 2010; Zhu and Wu, 2004), for example, the labeling error rate exceeds 4% in the natural scene image dataset ImageNet (Van Horn et al., 2015). Compared to natural scene images, the objects in remote sensing scene images have large orientation and scale variations (Cheng et al., 2014; Li et al., 2018), making it more difficult for annotators to assign a correct semantic label to each remote sensing scene image. Hence, understanding the impact of unavoidable human labeling errors on ConvNets is essential for improving their reliability in remote sensing image scene classification.

In general, labeling errors, also known as label noise, may bias the learning process, inevitably degrading the ConvNets and adversely affecting their accuracy (Frenay and Verleysen, 2014; Li et al., 2021; Nettleton et al., 2010). To explore the impact of labeling errors, corrupting a well-labeled dataset with simulated label noise is commonly used (Jiang et al., 2020). The simulated label noise is generally derived by flipping the true label to an incorrect class under some constraint. Two types of simulated label noise, namely uniform noise and class-dependent noise, are widely used (Zhu and Wu, 2004; Nettleton et al., 2010; Reed et al., 2015; Rolnick et al., 2018; Chen et al., 2019; Hendrycks et al., 2019; Jiang et al., 2019; Algan and Ulusoy, 2020; Jiang et al.,

2020; Elmes et al., 2020). Uniform noise assumes that the probability of error is independent of the true class itself. In this case, the true label is flipped to any other incorrect class with an equal likelihood. In contrast, class-dependent noise assumes that the probability of error depends on the true class, making simulations more realistic compared to uniform noise. Specifically, the true label is flipped to an incorrect class based on the probability defined by the inter-class similarities, resulting in the true label preferring to be corrupted to some incorrect classes. However, the inter-class flipping probabilities used in class-dependent noise are generally designed by randomization (Litany and Freedman, 2018) or empirically similar semantic categories (Hendrycks et al., 2018; Li et al., 2019; Patrini et al., 2017; Yi and Wu, 2019). Furthermore, class-dependent noise as well as uniform noise is independent of instances due to the completely random selection of the instances to be corrupted. In contrast, label noise in real conditions may be class-dependent, instance-dependent, or even adversarial (Jiang et al., 2019) and is likely to vary across annotators due to their various annotation skills. Therefore, understanding ConvNets on simulated label noise is not straightforwardly applicable to real-world tasks.

To inform how well ConvNets are expected to perform under real-world label noise, Jiang et al. (2020) established a benchmark of real-world label noise by injecting noisy web label to a well-labeled dataset (Mini-ImageNet and Stanford Cars) and reported the performance differences of ConvNets on noisy label across different noise levels; and Van Horn et al. (2015) measured the quality of two datasets including CUB-200-2011 and ImageNet, and the accuracy reduction caused by the label errors in these two datasets. However, due to the different label competences between untrained and trained annotators, the label noise in Jiang et al. (2020) obtained from the web composed of untrained annotators, may differ from the noise induced by well-trained annotators in real-world tasks. Moreover, in contrast to natural scene images, the large orientation and scale

variations of objects in remote sensing scene images (Cheng et al., 2014; Li et al., 2018) raise unique issues, making the labeling errors and their impact on ConvNets in the remote sensing image scene classification probably more severe or even adversarial. Finally, the previous studies lack explicit analysis of the impact of real-world label noise on supervised learning algorithms. Hence, there is a demand for systematically exploring the influence of real-world label noise on ConvNets.

Motivated by this, this study proposed to systematically evaluate the influence of real-world label noise on ConvNets for remote sensing scene classification. In particular, we collected real-world labels for a widely used dataset, UCMerced (Yang and Newsam, 2010), from 32 participants, and explored the influence of their labeling errors on the three typical ConvNets, namely VGG16 (Simonyan and Zisserman, 2015), GoogLeNet (Szegedy et al., 2015) and ResNet-50 (He et al., 2016). Here labeling error patterns were quantitatively evaluated first to clarify the need for datasets with real-world label noise. Then, relationships between human labeling errors and ConvNets errors were examined to analyze the consequences of real-world label noise. To provide insight into the influence of real-world label noise, we further compared human labeling errors with two widely used types of simulated label noise, namely uniform noise and class-dependent noise, which are generated based on human labeling error patterns.

The rest of this paper is organized as follows. Section 2 describes the datasets, behavioral experiment, comparative experiment with simulated labels and assessment of the impact of label errors on ConvNets. Section 3 presents and discusses the experimental results, followed by a conclusion in Section 4.

## **2. Materials and experimental design**

Our study includes three experiments as shown in Fig. 1 using 600 images from 6 categories in the dataset UCMerced. First, half of these images were used in a behavioral experiment to collect real-world labels from participants. Then human labels were used for training ConvNet models. The impact of human labeling errors was assessed from two dimensions, per participant and per error type. Finally, a comparative experiment was conducted for comparing the impact of human labels with that of simulated labels. The simulated labels were generated based on the patterns of human labeling errors.

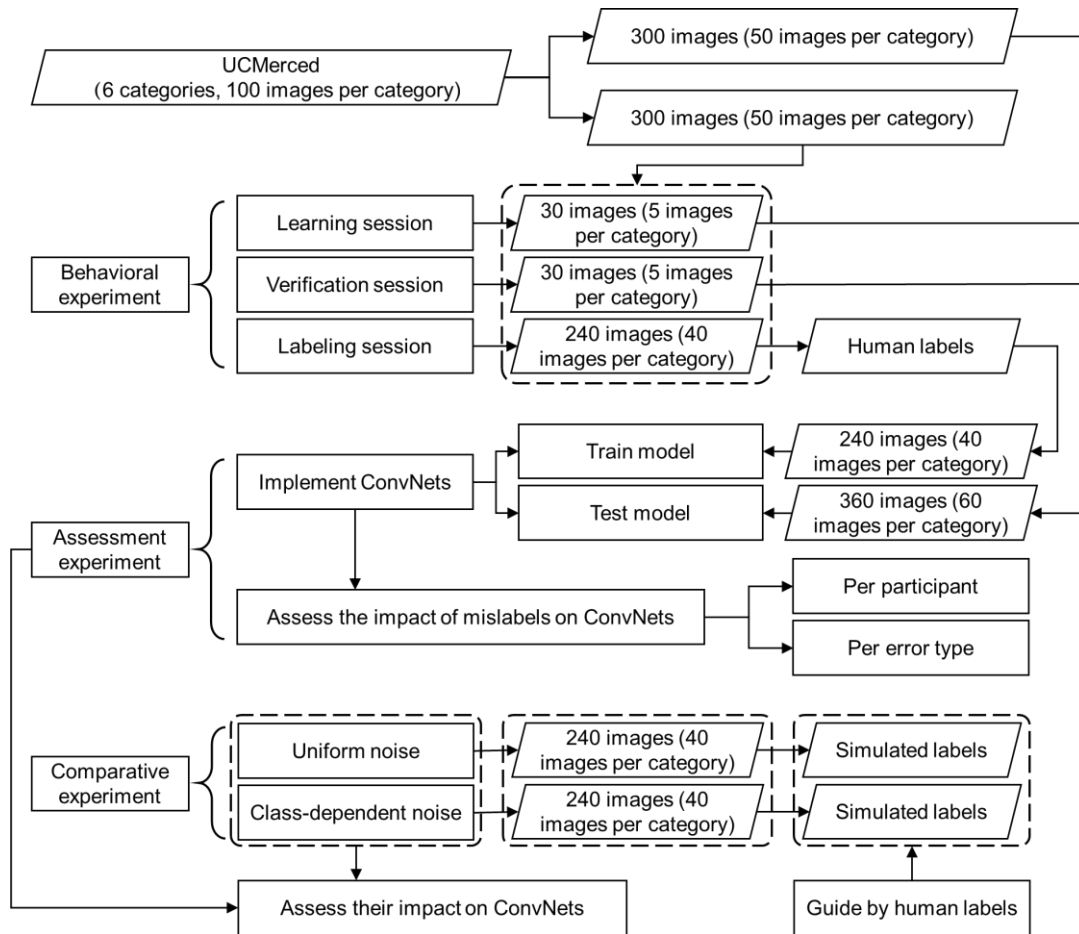


Fig. 1. Flowchart for the experiments.

## 2.1. Dataset

UCMerced land use dataset (Yang and Newsam, 2010), one of the most widely used datasets in remote sensing scene classification (Chen et al., 2022; Cheng et al., 2020, 2017; Dimitrovski et al., 2022; Ma et al., 2021; Nogueira et al., 2017; Yuan et al., 2022), was used in this study. It consists of 21 land-use classes over different US regions and 100 aerial RGB images for each category. Each satellite image scene has 256 by 256 pixels with a pixel resolution of one foot. Among the 2100 aerial images, we selected 600 images from 3 artificial categories (airplane, freeway and runway) and 3 nature categories (beach, forest and river) for the experimental study (Fig. 2).

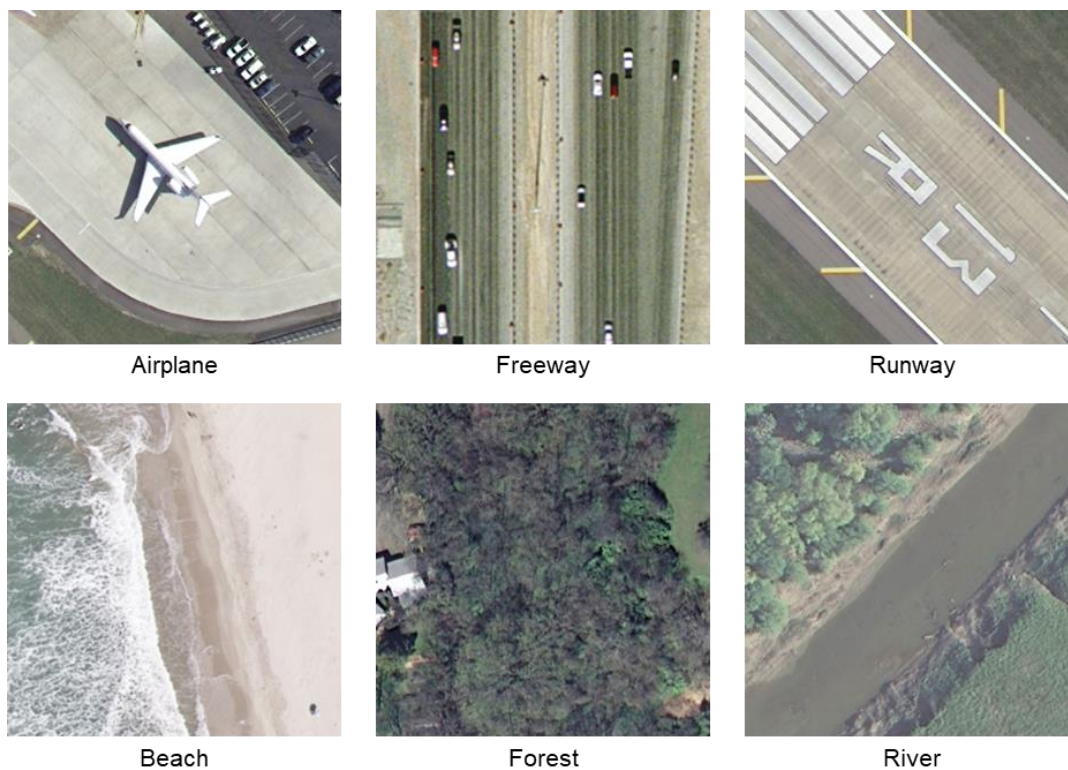


Fig. 2. Example images of six categories.

## 2.2. Behavioral experiment

In order to investigate the influence of human labeling errors on training ConvNets, we first conducted a behavioral experiment to obtain human labeling errors, where participants were trained with category labels of remote sensing images.

### *2.2.1. Participants*

32 participants participated in the behavioral experiments (18 females; mean age 20). All participants were recruited from Shenzhen University and had normal or corrected-to-normal vision. They signed an informed consent form prior to the experiment and were paid for their participation afterward.

### *2.2.2. Stimulus*

From UCMerced, 300 remote sensing images were selected from the six categories with 50 images per category. All images were randomly assigned to the learning, verification, and labeling sessions of 30 (5 images per category), 30 (5 images per category), and 240 (40 images per category) respectively.

### *2.2.3. Design and procedure*

Each experiment has three sessions: learning, verification, and labeling sessions. The first two sessions were completed in an online questionnaire platform ([www.wjx.cn](http://www.wjx.cn)) and the labeling session was tested on E-prime 3.0.

In the learning session, participants' task was to learn the relationship between remote sensing images and their category labels. On each trial, they were presented with an image with the category label. When they thought they had learned the relation, they pressed a button to proceed to the next trial. There was no time limit for learning. In this session, participants learned a total of 30 remote sensing images, five from one of six categories. The order of images was all randomized across participants.

In the verification session, participants were required to classify the remote sensing images using the category labels that they acquired in the learning session. On each trial, participants were presented with a remote sensing image with six category labels. If they chose the correct category label, they would move on to the next trial. Otherwise, the correct label would appear. Each trial had no time limit. There were 30 trials in total with five trials in each category. The purpose of this session was to give feedback to participants. If they were not satisfied with their performance, they could redo the learning session.

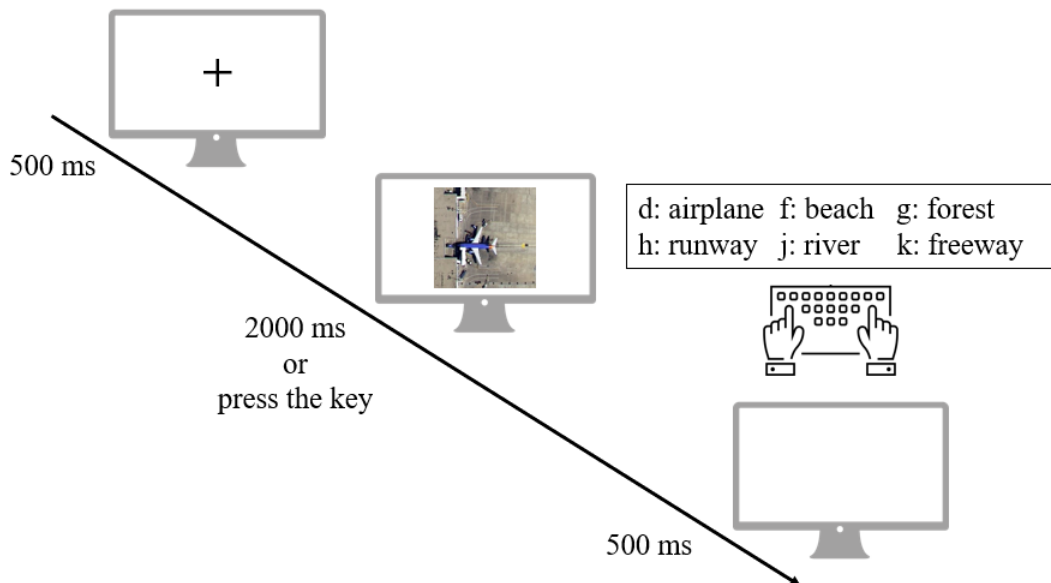


Fig. 3. The procedure of one trial in the labeling session

In the labeling session, participants were instructed to respond by pressing the corresponding key on the keyboard to classify the remote sensing images. A sheet of paper with six category labels and corresponding keys was placed on the desk to remind participants. As shown in Fig. 3, each trial began with a fixation point "+" in the center of the screen for 500ms. A remote sensing image followed immediately after the fixation point disappeared. Different from

the other sessions, the image disappeared as soon as participants pressed the key or it remained for 2000ms. Then, a blank screen appeared for 500ms and the next trial appeared. There were 40 images from each of the six categories, resulting in a total of 240 trials. This session lasted approximately 20 minutes. Participants' key presses and response times were recorded by E-prime 3.0.

#### *2.2.4 Behavioral data analysis*

To test whether human labeling errors were dependent on different categories (airplane, beach, forest, freeway, river, runway), the following linear mixed effects analyses were conducted in the R (version 4.2.1) using lme4 (version 1.1-31; Bates et al., 2015) to explore the relationship between error rates and category. Because pictures were nested within categories, we included this nested structure as a random effect in addition to participants (Bates et al., 2015). To test the main effect of category, we conducted likelihood ratio tests of the model with category as a fixed effect (full model) against the model without category (null model). To further test between which categories the error rates were significantly different, we conducted post-hoc contrast analyses with emmeans (version 1.8.5; Lenth, 2023).

### **2.3. Experiment of training ConvNets with human mislabels**

The 240 images associated with human labels (i.e., no-test set) were used for training ConvNets, whereas the remaining 360 images from the six selected categories formed the test set for evaluating the performance of ConvNets with correct labels.

Three typical ConvNets for scene classification, including VGG16 (Simonyan and Zisserman, 2015), GoogLeNet (Szegedy et al., 2015) and ResNet-50 (He et al., 2016), were selected for our experiment. These networks have been widely used as benchmarks for remote sensing scene classification and have shown great performance (Chen et al., 2022; Cheng et al., 2017;

Dimitrovski et al., 2022; Ma et al., 2021; Nogueira et al., 2017; Yuan et al., 2022). VGG16 has a simple architecture built by stacking multiple convolutional layers, max pooling layers and fully connected layers. GoogLeNet has not only a deep structure but also a wide structure that adopts multiple different convolutional filter sizes in parallel to process visual information at various scales. ResNet-50 adopts residual learning performed by shortcut connections to construct significantly deeper networks compared to the VGG family and GoogLeNet.

All the networks were implemented in PyTorch version 1.13.0 on an Ubuntu 9.4.0 system using 2 NVIDIA GeForce RTX 3090 GPUs. RAdam optimizer (Liu et al., 2021) with a learning rate of  $10^{-4}$  was used as the optimization algorithm for training. The batch size was fixed at 128, and the standard cross-entropy was used as the loss function (more details in Appendix 1.). A network was trained on the no-test set with human labels derived from a participant, thus resulting in a total of 32 copies for one of the three selected networks. The trained model was then evaluated on the test set with correct labels. To quantitatively measure the performance of the model, the overall accuracy (OA) (Stehman, 1997) was reported. It refers to the proportion of correctly classified instances to the total instances:

$$OA = \frac{\sum_{i=1}^6 N_{ii}}{\sum_{i=1}^6 N_i} \quad (1)$$

where  $N_{ii}$  denotes the number of instances belonging to category  $i$  and labeled as category  $i$ , and  $N_i$  denotes the number of instances belonging to category  $i$ .

Regarding the impact of label noise on ConvNets, we explored it from two dimensions, per participant and per error type. First, each participant made unique labeling errors on the no-test set which can be represented by an error matrix as shown in Fig. 4 (a). The non-diagonal elements in the matrix are specific type of errors made by the participant, which are relative error frequency calculated as:

$$F_{ij} = \frac{N_{ij}}{N_i}, i \neq j \quad (2)$$

where  $F_{ij}$  and  $N_{ij}$  is the relative frequency and the number of instances belonging to category  $i$  but mislabeled as category  $j$ , respectively, and  $N_i$  is the number of instances belonging to category  $i$ . The labels created by each participant were used to train ConvNet model and that trained model obtained its error matrix from the test dataset as shown in Fig. 4 (b). The first question is whether the error pattern made by each participant is propagated by the ConvNet mode. To answer this question, the error matrix of each participant and its corresponding ConvNet matrix were flattened and then a linear regression model was built between these two vectors (Fig. 4 (c)). The slope of this regression line indicates whether ConvNet model amplified the human labeling errors (slope  $>1$ ) or tolerated the human labeling errors (slope  $<1$ ). Testing hypotheses about the slopes were further proceeded for assessing the validity of the linear regressions. The resulting  $p$ -values were adjusted by the Benjamini-Hochberg FDR controlling procedure (Benjamini and Hochberg, 1995) to control the false discovery rate (FDR) for independent test statistics in multiple significance testing problems. To further investigate whether ConvNet model is affected by the overall accuracy of each participant, a regression model was built between the overall accuracies of all 32 participants and their corresponding ConvNet models (Fig. 4 (d)).

Second, for a specific error type, e.g., freeway images mislabeled as airplane, all participants may make such type of error but with different frequencies (Fig. 5 (a)). After training a ConvNet separately on no-test set with labels from 32 participants, 32 copies of a ConvNet with different parameters were evaluated on test set. As shown in Fig. 5, errors in participant labels, such as freeway mislabeled as runway, appeared in some copies of the ConvNet (Fig. 5 (b)). The second question is how ConvNet model reacts to a specific error type, whether it made the same error as participants or not. To answer this question, the relationship between labeling errors and

the corresponding ConvNet errors was analyzed for each error type (Fig. 5 (c)). The significance testings of the regression slopes were also proceeded and that resulting  $p$ -values were adjusted by the Benjamini-Hochberg FDR controlling procedure (Benjamini and Hochberg, 1995).

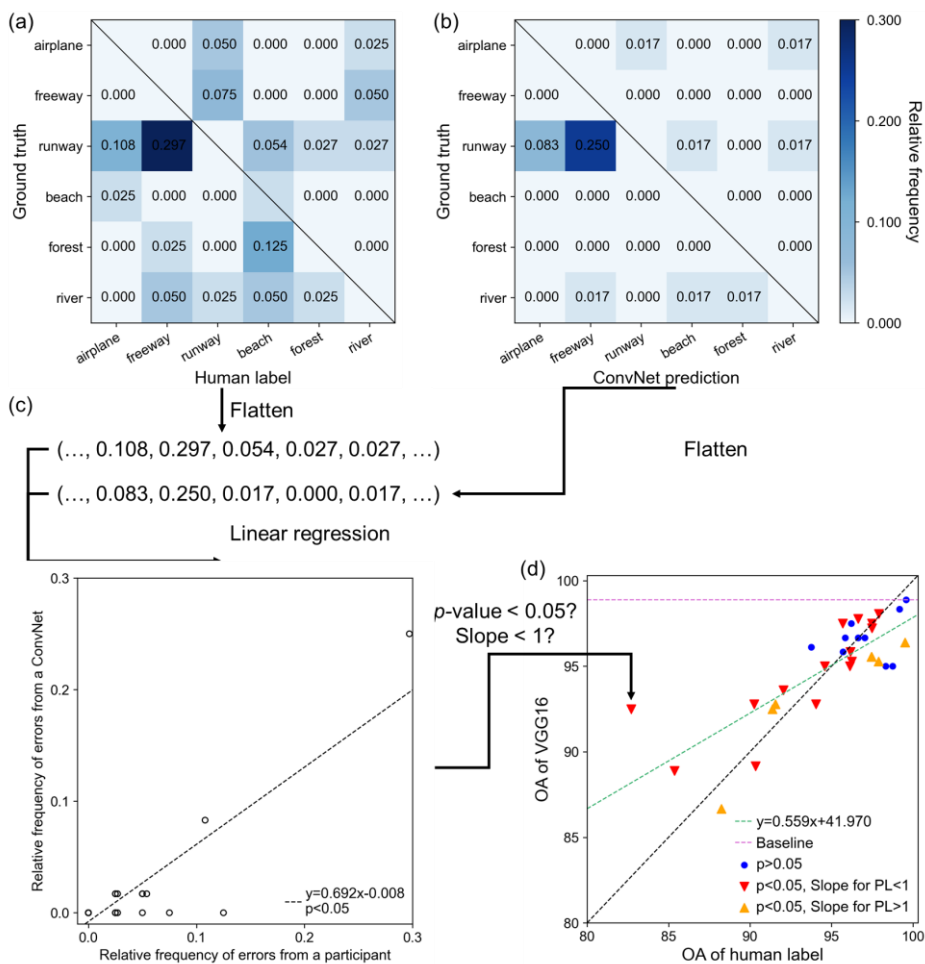


Fig. 4. Assessment of the impact of label noise on ConvNets for per participant. The error pattern of (a) the first participant on no-test set and (b) the corresponding trained ConvNet on test set. The number in each entry represents the relative frequency of incorrectly classified instances. (c) Participant-level assessment for the first participant. Linear regression analysis was performed between the labeling errors in (a) and the corresponding ConvNet errors in (b) to assess the impact of participant labeling errors on ConvNet. This procedure was repeated for each participant. The

$p$ -value and slope in the assessment for each participant are expressed by the scatter styles in (d) that describes the changes in the OA of a ConvNet as the OA of human labels changes. The green dash line denotes the trend in test accuracy of ConvNets versus the accuracy of participant's labels. The baseline represents the model trained on a labeling-error free scenario.

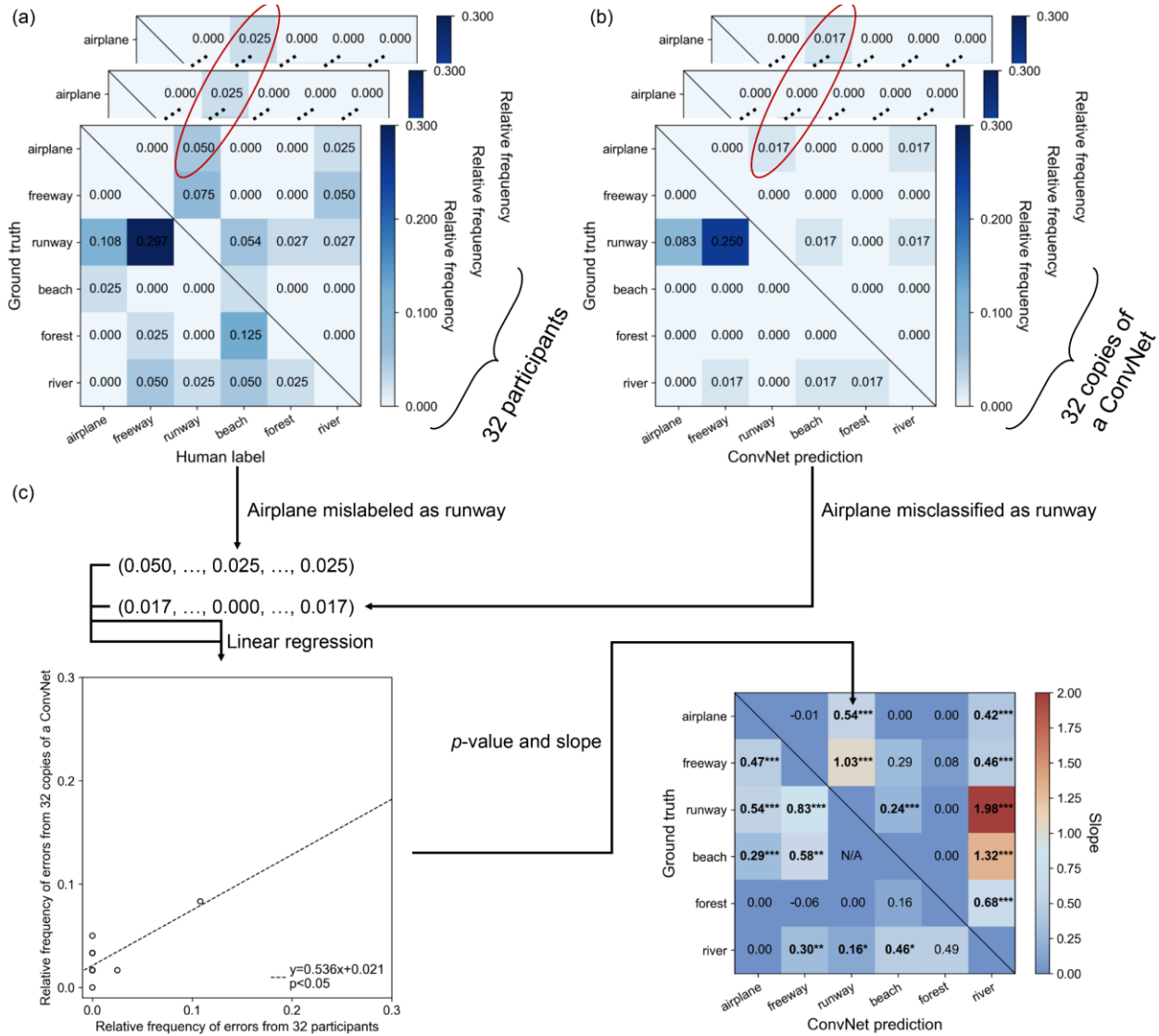


Fig. 5. Assessment of the impact of label noise on ConvNets for per error type. The error pattern of (a) 32 participants on no-test set and (b) the corresponding 32 copies of a ConvNet on test set. The number in each entry represents the relative frequency of incorrectly classified instances. (c)

Error type-level assessment for the specific error type where airplane misclassified as runway. Linear regression analysis for this error type was performed between 32 participants and the corresponding ConvNets to assess how ConvNet reacts to this error type. This procedure was repeated for each error type.

## 2.4. Comparative experiment with simulated mislabels

To elucidate the mechanism underlying the impact of real-world label noise on ConvNets, two types of simulated label noise, namely, uniform noise and class-dependent noise, were modeled for each participant based on his/her error pattern and compared to human labeling errors. These simulated labels with label noise were generated for the 240 images in the labeling session of the behavioral experiment (section 2.2.3).

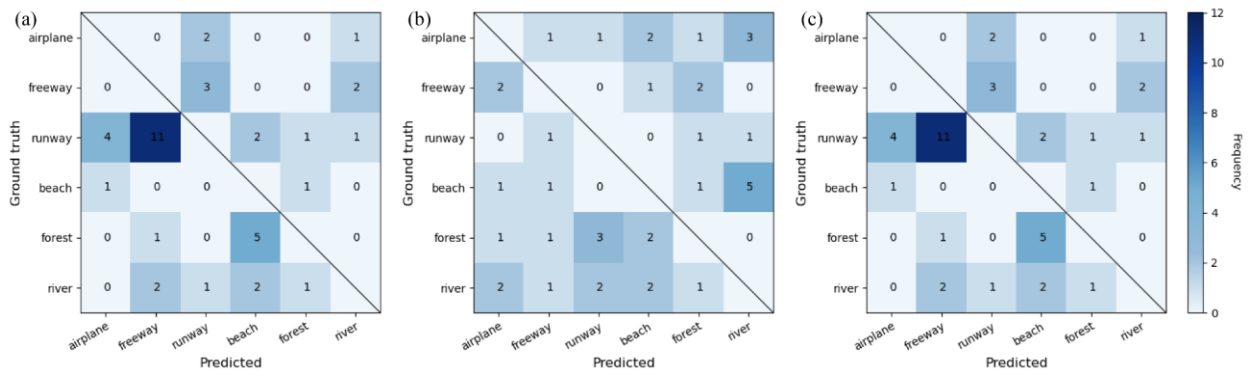


Fig. 6. Illustration of two types of simulated label noise. (a) The error pattern of the first participant. The noise patterns of (b) uniform noise and (c) class-dependent noise, both of which are modeled based on (a). The number in each entry represents the frequency of incorrectly classified instances.

Uniform noise is generated by randomly selecting instances and then flipping their correct labels to random labels from a uniform distribution over the other remaining labels, resulting in simulated label noise being instance-independent and approximately uniformly distributed over all

error types (Fig. 6 (b)). For each participant, the number of the selected instances is the same as the frequency of the participant labeling errors, remaining label noise ratio unchanged.

Class-dependent noise is generated by counting the frequency of each error type for each category, randomly selecting instances in this category, and flipping their correct labels to incorrect labels randomly obtained from the counted errors, resulting in that simulated label noise is instance-independent and maintains a consistent pattern with participant labeling errors (Fig. 6 (c)). For each participant, the number of the selected instances for each category is the same as the frequency of this participant labeling errors of the same category, remaining label noise ratio for each category unchanged.

These two types of simulated label noise were performed 30 times for each participant to consider the random effect of the sample selection and label flipping. These simulated labels were used to train the three ConvNets and assess their performance in the test set as described in Section 2.3. We analyzed how they influence the ConvNets and compared their impact with that of human labeling errors.

### **3. Results and discussion**

#### **3.1. Noise pattern of human labeling errors**

Table 1 shows the results of linear mixed effects analyses with category as a fixed effect. Adding Category to the model significantly improved Model fitting ( $p < .001$ ), suggesting that participants made more errors in some categories than others. Post-hoc contrast analyses further showed that the error rate of airplane is lower than all categories except beach, and the error rate of beach is lower than freeway and river (Table 2). There are no significant differences between other categories.

Table 1. The result of model comparison.

Model	Random effect	Fixed effect	AIC	BIC	LogLik	Dev	X <sup>2</sup>	df	p
Null model	(1 Subject)	-	3561.7	3582.6	-1777.9	3555.7			
Full model	+(1 Category /Picture)	Category	3416.9	3479.4	-1699.5	3398.9	156.85	6	< 2.2e-16***

\*  $p < .05$ , \*\*  $p < .01$ , \*\*\*  $p < .001$

Table 2. The result of post hoc multiple comparisons.

Contrast	b	SE	z	p
airplane-beach	-0.58	0.29	-1.99	.35
airplane-forest	-1.29	0.28	-4.61	.0001***
airplane-freeway	-1.63	0.27	-5.94	<.0001***
airplane-river	-1.36	0.28	-4.90	<.0001***
airplane-runway	-1.21	0.28	-4.33	.0002***
beach-forest	-0.70	0.26	-2.76	.06
beach-freeway	-1.05	0.25	-4.19	.0004***
beach-river	-0.78	0.25	-3.07	.03*
beach-runway	-0.63	0.26	-2.46	.14
forest-freeway	-0.34	0.23	-1.48	.68
forest-river	-0.08	0.24	-0.32	.99
forest-runway	0.07	0.24	0.309	.99
freeway-river	0.27	0.23	1.156	.86
freeway-runway	0.42	0.23	1.787	.47
river-runway	0.15	0.24	0.629	.99

\*  $p < .05$ , \*\*  $p < .01$ , \*\*\*  $p < .001$  (the  $p$ -value of post hoc multiple comparisons was adjusted by Tukey test)

To investigate whether the main effect of category is due to specific pictures, we calculated the mean error rate of each picture within a category. As shown in the boxplots on Fig. 7, outliers have been identified for all categories except for beach, suggesting that participants were more likely to make error on some pictures than others.

In sum, participants' errors were affected by both categories and pictures, demonstrating the errors made by them were not random.

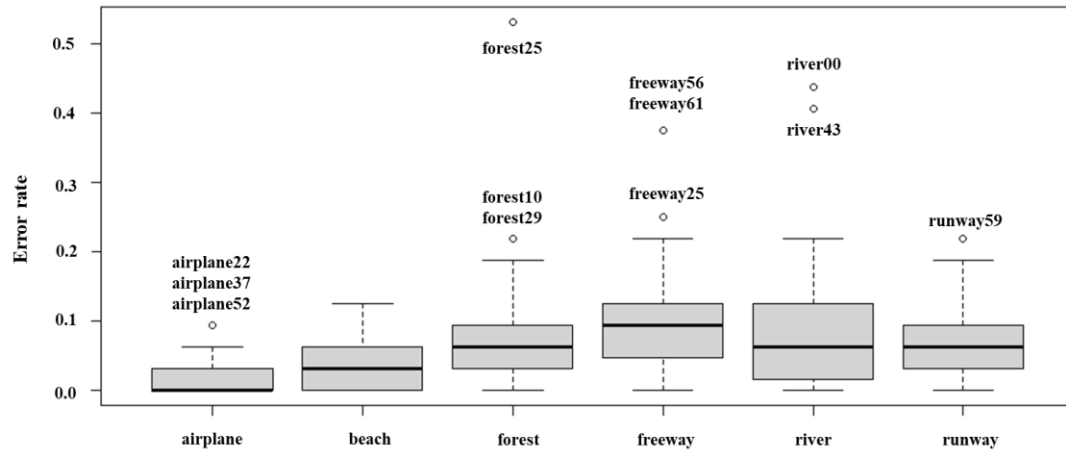


Fig. 7. The boxplots of human labeling errors in each category.

### 3.2. Impact of human labeling errors on ConvNets

We collected real-world labels from 32 participants and trained a ConvNet with the labels of each participant. The procedure yielded 32 copies of ConvNet for each of the three ConvNets (VGG16, GoogLeNet and ResNet-50). ConvNets performed better than participants in classifying remote sensing images. The average human accuracy on no-test set was 94.9% (s.e.=4.0%), in comparison to test accuracies of 95.0% (s.e.=3%), 97.7% (s.e.=2%) and 97.6% (s.e.=2%) for VGG16, GoogLeNet and ResNet-50 on test set, respectively. When the human accuracy decreased by one unit, the test accuracy of ConvNets decreased by around half a unit (Fig. 8). For the baseline comparison, ConvNets trained with labeling errors were able to achieve comparable or even better performance compared to the baseline model trained without labeling errors. This suggests that ConvNets are able to handle human labeling errors and achieve higher overall performances than humans in remote sensing scene classification. Regarding each participant, labeling errors for about half of the participants were significantly correlated with ConvNet errors (the triangle

scatters in Fig. 8). In this case, most of the changes in ConvNet errors for a one-unit change in labeling errors were less than one unit (Fig. 9). This indicates that ConvNets tolerate human labeling errors in most cases in remote sensing scene classification.

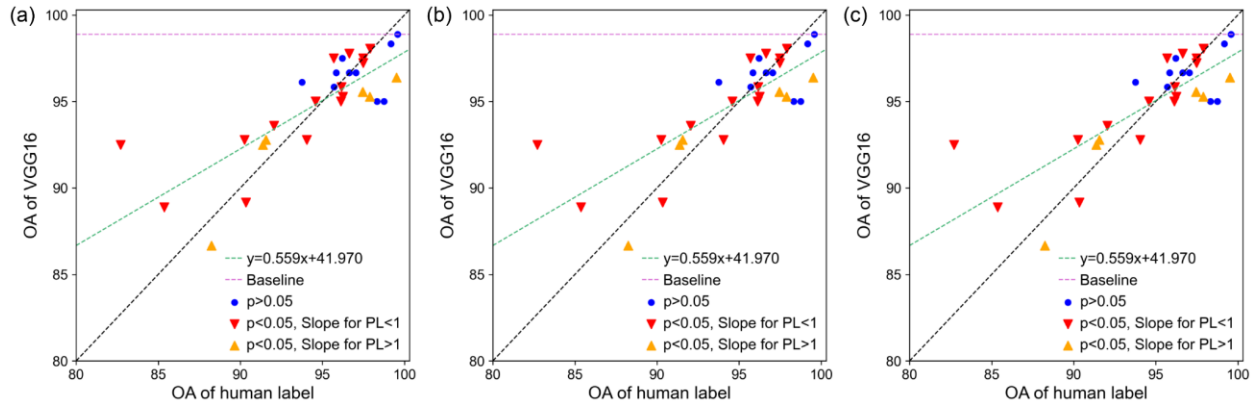


Fig. 8. Test accuracy of various copies of (a) VGG16, (b) GooLeNet and (c) ResNet-50 under labeling errors from different participants, as well as participant-level assessment results for all 32 participants (expressed by the scatter styles). The baseline represents the model trained on a label-error free scenario.

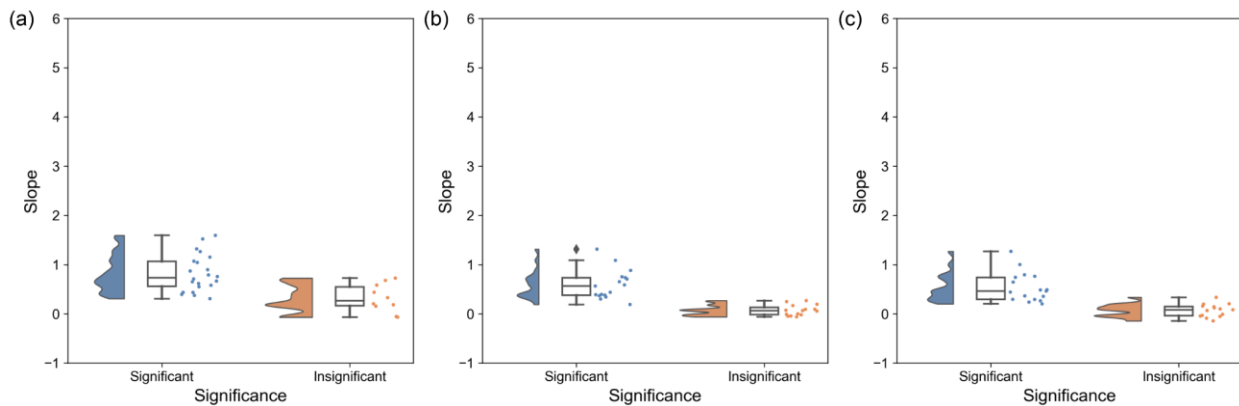


Fig. 9. The raincloud plot of slopes of the linear regression between participant labeling errors and ConvNet errors for each participant. (a) VGG16, (b) GooLeNet and (c) ResNet-50.

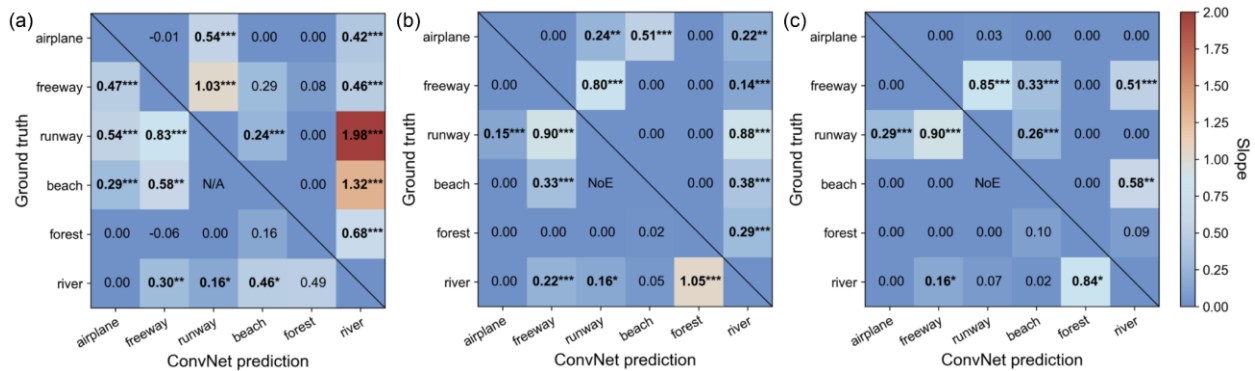


Fig. 10. Error type-level assessment results for all 30 error types for (a) VGG16, (b) GoogLeNet and (c) ResNet-50. The number in each entry represents the slope of the linear regression of the ConvNet errors onto the corresponding human labeling errors across all participants. The bold text denotes a significant linear relation. \*, \*\* and \*\*\* denote that the linear regression is statistically significant at the level of  $p < 0.05$ ,  $p < 0.01$  and  $p < 0.001$ , respectively. The  $p$ -value was corrected by the Benjamini-Hochberg FDR controlling procedure. N/A denotes that there is no slope since the error type is not present in no-test set but occurs in ConvNet predictions. NoE denotes that there is no slope since the error type is not present in either no-test set or ConvNet predictions.

For each error type, the vast majority of all 30 error types were tolerated by ConvNets. Although for about half of all error types, the labeling errors from 32 participants were insignificantly correlated with the same type of errors from ConvNets, the slopes of these correlations were mostly close to 0 (Fig. 10), indicating that a one-unit increase in these types of labeling errors produces few increases in ConvNet errors. For the remaining error type, labeling errors were significantly correlated with ConvNets errors. As labeling errors for most of these error types increased by one unit, ConvNets errors increased by less than one unit (Fig. 10). These suggest that ConvNets generally tolerate the category impact of human labeling errors.

### 3.3. Comparison of impact from human labeling errors and simulated label noise

To uncover the mechanism of the impact of human labeling errors, we compared it to simulated label noise. We modeled uniform noise and class-dependent noise 30 times each and evaluated their impact on ConvNets. Both uniform noise and class-dependent noise were modeled based on the participants' error patterns. Class-dependent noise was more impactful than uniform noise but has an impact similar to human labeling errors. A 1% drop in the accuracy of labels corrupted by class-dependent noise reduced the accuracy of ConvNets by around 0.5%, which was larger than the decrease caused by uniform noise but similar to that caused by human labeling errors (Fig. 11). For each simulation for each participant, an increase of one unit in the label noise mostly increased ConvNet error by less than one unit (Fig. 12), indicating the robustness of ConvNets on both two types of simulated label noise. However, the simulated label noise significantly correlated with ConvNet errors occurred more often in simulations of class-dependent noise than in simulations of uniform noise (Fig. 12). Furthermore, there are fewer simulations of uniform noise that was significantly amplified by ConvNet compared to simulations of class-dependent noise (Fig. 12). These results suggest that class-dependent noise brings more challenge than uniform noise to ConvNets and the impact of human labeling errors on ConvNets may stem from the class-dependent characteristic.

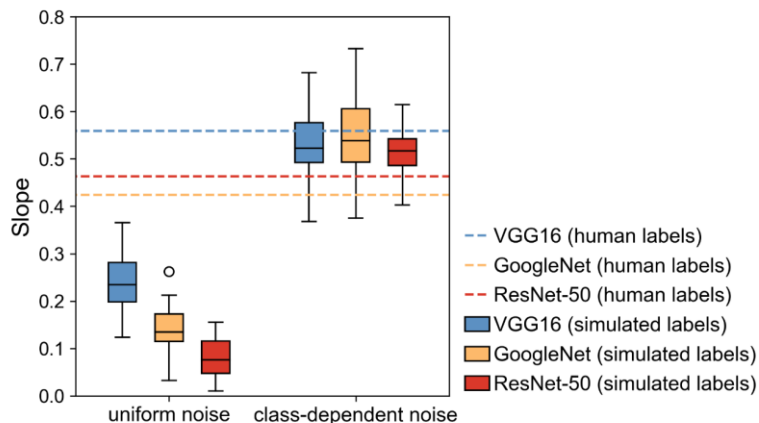


Fig. 11. The slopes of the linear regression between the OA of ConvNets onto the OA of the corresponding human (lines) and simulated labels (box plots).

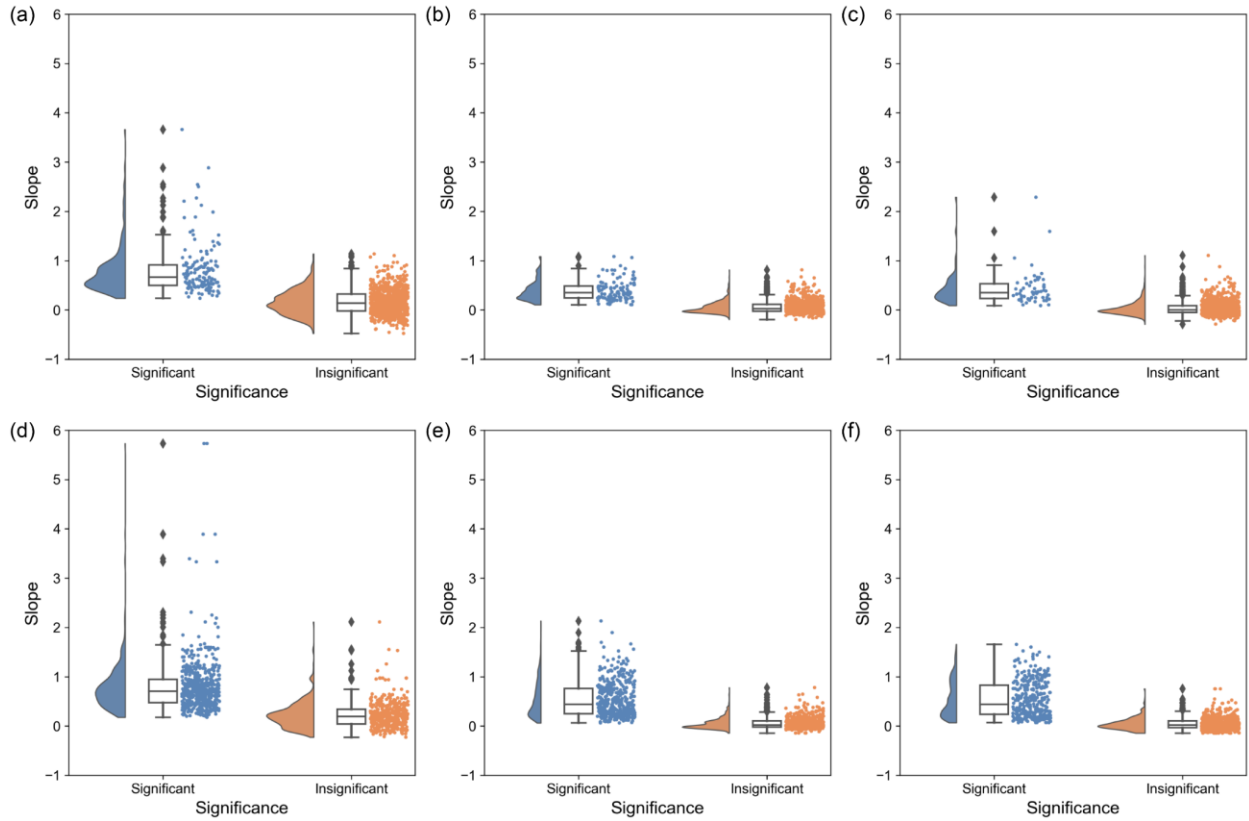


Fig. 12. The raincloud plot of slopes of the linear regression between participant labeling errors and ConvNet errors for each participant’s simulation. (a) VGG16, (b) GooLeNet and (c) ResNet-50 trained with uniform noise; (d) VGG16, (e) GoogLeNet and (f) ResNet-50 trained with class-dependent noise.

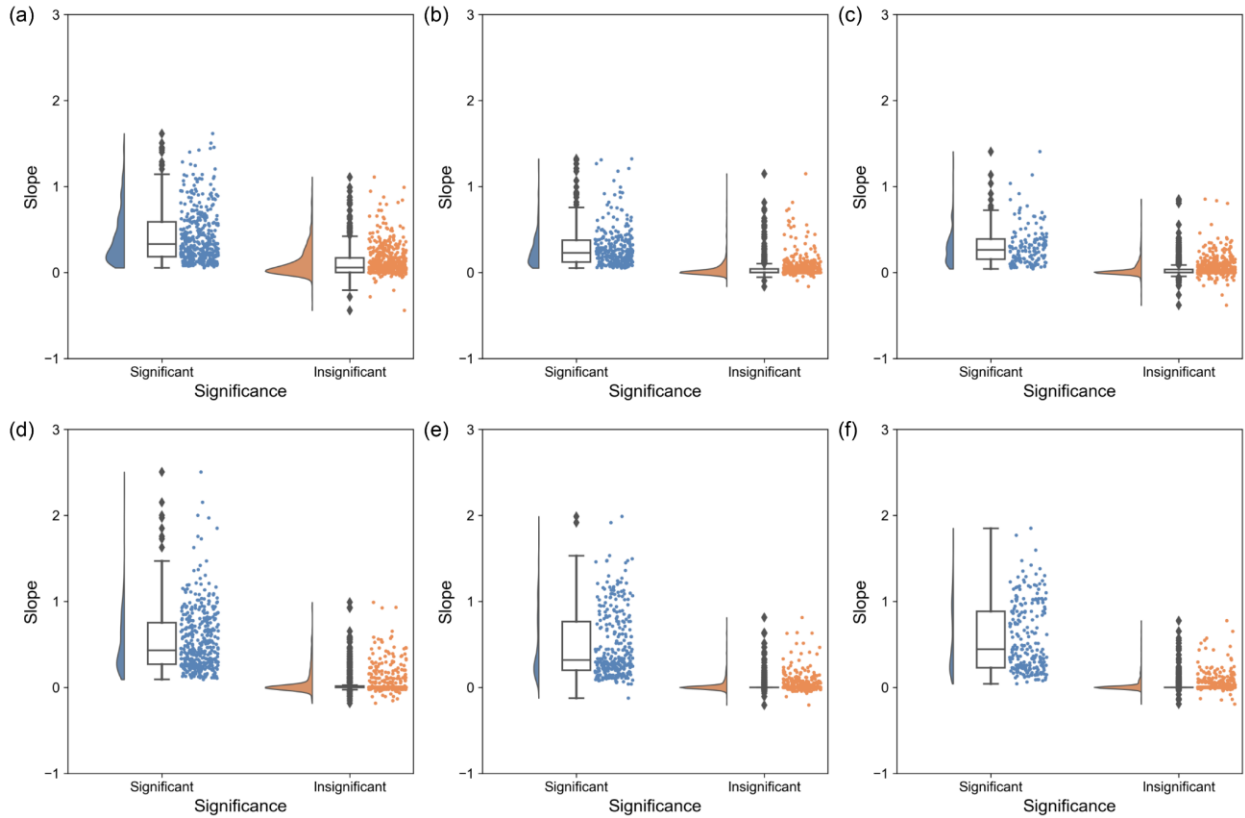


Fig. 13. The raincloud plot of slopes of the linear regression between participant labeling errors and ConvNet errors over each error type. (a) VGG16, (b) GooLeNet and (c) ResNet-50 trained with uniform noise; (d) VGG16, (e) GoogLeNet and (f) ResNet-50 trained with class-dependent noise.

Regarding each error type, simulated noise of the vast majority of error types was tolerated by ConvNets. For the error types where the correlations between ConvNet errors and simulated label noise were insignificant, slopes of linear regression lines of these correlations were mostly around 0 (Fig. 13), indicating that each one unit increase in simulated noise for each of these error types caused almost no increase in ConvNet errors. Such correlations for the remaining error types were significant and mostly had a line with a slope less than 1 (Fig. 13). These results suggest that

the category impact of the two types of simulated label noise was generally tolerated by ConvNets, similar to the findings on human labeling errors.

#### **4. Conclusion**

In this study, we conducted a behavioral experiment to obtain human labeling errors from well-trained participants and systematically explored the impact of real-world labeling errors on ConvNets for remote sensing scene classification. We found that participants' labeling errors were significantly related to categories and instances. When training ConvNets with these participants' labels, human mislabels can significantly affect the performance of ConvNets but that impact shows high heterogeneity among classes. We further compared human labeling errors with simulated label noise, including uniform noise and class-dependent noise. The results showed that human labeling errors had an impact similar to class-dependent noise rather than uniform noise. Considering that class-dependent noise differs from human labeling errors in the mislabeled instances, the instance dependence in human labeling errors affects ConvNets relatively little. Furthermore, class-dependent noise is more challenging than uniform noise mainly due to the heterogeneity of the number of mislabeled instances over occurring error types. Hence, we recommend that creating a dataset of label noise based on a class-dependent noise pattern would be closer to a real-world scenario, which benefits the evaluations and applications of algorithms in real-world tasks. In addition, due to the difficulties of obtaining a real-world class-dependent noise pattern, how to simulate a real label noise remains a challenge.

#### **Acknowledgments**

This study was supported by Shenzhen Higher Institution Stability Support Plan (20200812154629001) and the Hong Kong Polytechnic University (project Nos. 1-ZVN6 and 4-ZZND).

## **Appendix**

### **1. Implementation details of ConvNets**

The training process for each network has two phases. In the first phase, the no-test set was randomly split into a training set for model training (that is, 75% of the images) and a validation set (that is, 25% of the images) for model validation. The network was initialized with the pretrained weights in ImageNet and then trained on the training set with a learning scheduler ReduceLROnPlateau. This learning scheduler reduces the learning rate by a factor when a metrics quantity has stopped improving for a ‘patience’ number of epochs. In our experiments, the metrics quantity was set to the validation loss, with a patience set to 5, a reduction factor set to 0.1 and a lower bound on the learning rate set to  $10^{-6}$ . Subsequently, the number of epochs was determined by the performance of the network on the validation set. The optimal number of epochs as well as learning rate changes were tracked and recorded for retraining the network in the second phase.

In the second phase, to fully exploit the limited instances with human labels, the entire no-test set was used to retrain each network with the hyperparameters recorded in the first phase. Specifically, the update of the network followed the same learning rate changes as the first phase and stopped at the same optimal number of epochs as the first phase.

### **References**

- Algan, G., Ulusoy, İ., 2020. Label Noise Types and Their Effects on Deep Learning.
- Ball, J.E., Anderson, D.T., Chan, C.S., 2017. Comprehensive survey of deep learning in remote sensing: theories, tools, and challenges for the community. *J. Appl. Remote Sens.* 11, 1. <https://doi.org/10.1117/1.JRS.11.042609>

- Benjamini, Y., Hochberg, Y., 1995. Controlling the False Discovery Rate: A Practical and Powerful Approach to Multiple Testing. *J. R. Stat. Soc. Ser. B Methodol.* 57, 289–300.  
<https://doi.org/10.1111/j.2517-6161.1995.tb02031.x>
- Chen, P., Liao, B., Chen, G., Zhang, S., 2019. Understanding and Utilizing Deep Neural Networks Trained with Noisy Labels.
- Chen, W., Ouyang, S., Tong, W., Li, X., Zheng, X., Wang, L., 2022. GCSANet: A Global Context Spatial Attention Deep Learning Network for Remote Sensing Scene Classification. *IEEE J. Sel. Top. Appl. Earth Obs. Remote Sens.* 15, 1150–1162.  
<https://doi.org/10.1109/JSTARS.2022.3141826>
- Cheng, G., Han, J., Lu, X., 2017. Remote Sensing Image Scene Classification: Benchmark and State of the Art. *Proc. IEEE* 105, 1865–1883.  
<https://doi.org/10.1109/JPROC.2017.2675998>
- Cheng, G., Han, J., Zhou, P., Guo, L., 2014. Multi-class geospatial object detection and geographic image classification based on collection of part detectors. *ISPRS J. Photogramm. Remote Sens.* 98, 119–132. <https://doi.org/10.1016/j.isprsjprs.2014.10.002>
- Cheng, G., Xie, X., Han, J., Guo, L., Xia, G.-S., 2020. Remote Sensing Image Scene Classification Meets Deep Learning: Challenges, Methods, Benchmarks, and Opportunities. *IEEE J. Sel. Top. Appl. Earth Obs. Remote Sens.* 13, 3735–3756.  
<https://doi.org/10.1109/JSTARS.2020.3005403>
- Dimitrovski, I., Kitanovski, I., Kocev, D., Simidjievski, N., 2022. Current Trends in Deep Learning for Earth Observation: An Open-source Benchmark Arena for Image Classification.

- Elmes, A., Alemohammad, H., Avery, R., Caylor, K., Eastman, J., Fishgold, L., Friedl, M., Jain, M., Kohli, D., Laso Bayas, J., Lunga, D., McCarty, J., Pontius, R., Reinmann, A., Rogan, J., Song, L., Stoyanova, H., Ye, S., Yi, Z.-F., Estes, L., 2020. Accounting for Training Data Error in Machine Learning Applied to Earth Observations. *Remote Sens.* 12, 1034. <https://doi.org/10.3390/rs12061034>
- Frenay, B., Verleysen, M., 2014. Classification in the Presence of Label Noise: A Survey. *IEEE Trans. Neural Netw. Learn. Syst.* 25, 845–869. <https://doi.org/10.1109/TNNLS.2013.2292894>
- He, K., Zhang, X., Ren, S., Sun, J., 2016. Deep residual learning for image recognition, in: *Proceedings of the IEEE Conference on Computer Vision and Pattern Recognition*. pp. 770–778.
- Hendrycks, D., Lee, K., Mazeika, M., 2019. Using Pre-Training Can Improve Model Robustness and Uncertainty.
- Hendrycks, D., Mazeika, M., Wilson, D., Gimpel, K., 2018. Using trusted data to train deep networks on labels corrupted by severe noise. *Adv. Neural Inf. Process. Syst.* 31.
- Jiang, J., Ma, J., Wang, Z., Chen, C., Liu, X., 2019. Hyperspectral Image Classification in the Presence of Noisy Labels. *IEEE Trans. Geosci. Remote Sens.* 57, 851–865. <https://doi.org/10.1109/TGRS.2018.2861992>
- Jiang, L., Huang, D., Liu, M., Yang, W., 2020. Beyond Synthetic Noise: Deep Learning on Controlled Noisy Labels.
- Kang, X., Duan, P., Xiang, X., Li, S., Benediktsson, J.A., 2018. Detection and Correction of Mislabeled Training Samples for Hyperspectral Image Classification. *IEEE Trans. Geosci. Remote Sens.* 56, 5673–5686. <https://doi.org/10.1109/TGRS.2018.2823866>

- Khan, A., Sohail, A., Zahoor, U., Qureshi, A.S., 2020. A survey of the recent architectures of deep convolutional neural networks. *Artif. Intell. Rev.* 53, 5455–5516.  
<https://doi.org/10.1007/s10462-020-09825-6>
- Khan, S., Naseer, M., Hayat, M., Zamir, S.W., Khan, F.S., Shah, M., 2022. Transformers in Vision: A Survey. *ACM Comput. Surv.* 54, 1–41. <https://doi.org/10.1145/3505244>
- Li, J., Wong, Y., Zhao, Q., Kankanhalli, M.S., 2019. Learning to learn from noisy labeled data, in: *Proceedings of the IEEE/CVF Conference on Computer Vision and Pattern Recognition*. pp. 5051–5059.
- Li, K., Cheng, G., Bu, S., You, X., 2018. Rotation-Insensitive and Context-Augmented Object Detection in Remote Sensing Images. *IEEE Trans. Geosci. Remote Sens.* 56, 2337–2348.  
<https://doi.org/10.1109/TGRS.2017.2778300>
- Li, Y., Zhang, Y., Zhu, Z., 2021. Error-Tolerant Deep Learning for Remote Sensing Image Scene Classification. *IEEE Trans. Cybern.* 51, 1756–1768.  
<https://doi.org/10.1109/TCYB.2020.2989241>
- Litany, O., Freedman, D., 2018. Soseleto: A unified approach to transfer learning and training with noisy labels. *ArXiv Prepr. ArXiv180509622*.
- Liu, B., 2011. Supervised Learning, in: *Web Data Mining*. Springer Berlin Heidelberg, Berlin, Heidelberg, pp. 63–132. [https://doi.org/10.1007/978-3-642-19460-3\\_3](https://doi.org/10.1007/978-3-642-19460-3_3)
- Liu, L., Jiang, H., He, P., Chen, W., Liu, X., Gao, J., Han, J., 2021. On the Variance of the Adaptive Learning Rate and Beyond. <https://doi.org/10.48550/arXiv.1908.03265>
- Ma, A., Wan, Y., Zhong, Y., Wang, J., Zhang, L., 2021. SceneNet: Remote sensing scene classification deep learning network using multi-objective neural evolution architecture

- search. *ISPRS J. Photogramm. Remote Sens.* 172, 171–188.  
<https://doi.org/10.1016/j.isprsjprs.2020.11.025>
- Nettleton, D.F., Orriols-Puig, A., Fornells, A., 2010. A study of the effect of different types of noise on the precision of supervised learning techniques. *Artif. Intell. Rev.* 33, 275–306.  
<https://doi.org/10.1007/s10462-010-9156-z>
- Nogueira, K., Penatti, O.A.B., dos Santos, J.A., 2017. Towards better exploiting convolutional neural networks for remote sensing scene classification. *Pattern Recognit.* 61, 539–556.  
<https://doi.org/10.1016/j.patcog.2016.07.001>
- Patrini, G., Rozza, A., Krishna Menon, A., Nock, R., Qu, L., 2017. Making deep neural networks robust to label noise: A loss correction approach, in: *Proceedings of the IEEE Conference on Computer Vision and Pattern Recognition*. pp. 1944–1952.
- Reed, S., Lee, H., Anguelov, D., Szegedy, C., Erhan, D., Rabinovich, A., 2015. Training Deep Neural Networks on Noisy Labels with Bootstrapping.
- Rolnick, D., Veit, A., Belongie, S., Shavit, N., 2018. Deep Learning is Robust to Massive Label Noise.
- Simonyan, K., Zisserman, A., 2015. Very Deep Convolutional Networks for Large-Scale Image Recognition.
- Stehman, S.V., 1997. Selecting and interpreting measures of thematic classification accuracy. *Remote Sens. Environ.* 62, 77–89. [https://doi.org/10.1016/S0034-4257\(97\)00083-7](https://doi.org/10.1016/S0034-4257(97)00083-7)
- Szegedy, C., Liu, W., Jia, Y., Sermanet, P., Reed, S., Anguelov, D., Erhan, D., Vanhoucke, V., Rabinovich, A., 2015. Going deeper with convolutions, in: *Proceedings of the IEEE Conference on Computer Vision and Pattern Recognition*. pp. 1–9.

- Van Horn, G., Branson, S., Farrell, R., Haber, S., Barry, J., Ipeirotis, P., Perona, P., Belongie, S., 2015. Building a bird recognition app and large scale dataset with citizen scientists: The fine print in fine-grained dataset collection, in: 2015 IEEE Conference on Computer Vision and Pattern Recognition (CVPR). Presented at the 2015 IEEE Conference on Computer Vision and Pattern Recognition (CVPR), IEEE, Boston, MA, USA, pp. 595–604. <https://doi.org/10.1109/CVPR.2015.7298658>
- Wu, X., 1995. Knowledge acquisition from databases. Intellect books.
- Yang, Y., Newsam, S., 2010. Bag-of-visual-words and spatial extensions for land-use classification, in: Proceedings of the 18th SIGSPATIAL International Conference on Advances in Geographic Information Systems - GIS '10. Presented at the the 18th SIGSPATIAL International Conference, ACM Press, San Jose, California, p. 270. <https://doi.org/10.1145/1869790.1869829>
- Yi, K., Wu, J., 2019. Probabilistic end-to-end noise correction for learning with noisy labels, in: Proceedings of the IEEE/CVF Conference on Computer Vision and Pattern Recognition. pp. 7017–7025.
- Yuan, J., Ru, L., Wang, S., Wu, C., 2022. WH-MAVS: A Novel Dataset and Deep Learning Benchmark for Multiple Land Use and Land Cover Applications. *IEEE J. Sel. Top. Appl. Earth Obs. Remote Sens.* 15, 1575–1590. <https://doi.org/10.1109/JSTARS.2022.3142898>
- Zhu, X., Wu, X., 2004. Class noise vs. attribute noise: A quantitative study. *Artif. Intell. Rev.* 22, 177.